Depth-varying azimuthal anisotropy and mantle flow in the Patagonian slab window

Hannah F. Mark [ID] * [1,2], **Douglas A. Wiens** [ID] [3], **Walid Ben-Mansour** [ID] [3], **Zhengyang Zhou** [ID][4]

[1]Department of Geology and Geophysics, Woods Hole Oceanographic Institution, Woods Hole, MA, USA, [2]Lamont Doherty Earth Observatory of Columbia University, Palisades, NY, USA, [3]Department of Earth, Environmental, and Planetary Sciences, Washington University in St. Louis, St. Louis, MO, USA, [4]College of Earth, Ocean, and Atmospheric Sciences, Oregon State University, Corvallis, OR, USA

Abstract   Subduction of spreading ridges forms slab windows which perturb the local structure and dynamics of the upper mantle. Slab windows may alter the pattern of mantle flow and serve as portals for the exchange of mantle material between upper mantle reservoirs that are otherwise separated by the boundary of the subducting slab. Here, we use Rayleigh waves to derive an azimuthally anisotropic regional seismic velocity model for the Patagonian slab window and use the anisotropy model to infer patterns of upper mantle flow and deformation. Anisotropic fast directions are primarily trench-parallel in the upper ~40 km of the mantle throughout the region, likely reflecting the history of subduction and compression along the South American margin. At greater depths sensed by long-period Rayleigh waves, fast directions within the youngest part of the slab window are consistent with cross-basin mantle flow between the Atlantic and Pacific, as previously suggested by shear wave splits. Overall, the anisotropic velocity model reveals complex, depth-dependent patterns of mantle deformation and flow within the Patagonian slab window.

1   Introduction

Slab windows, formed when a ridge subducts and opens a gap in the subducting plate interface, are distinctive and dynamic tectonic environments (e.g., Thorkelson, 1996). Slab windows are associated with high surface heat flow (Ávila and Dávila, 2018); a lack of seismicity and typical arc volcanism (Agurto-Detzel et al., 2014; DeLong et al., 1979); and adakitic volcanism above subducting slab edges (Bourgois et al., 2016; Stern and Kilian, 1996). Seismic events and arc volcanoes are absent because there is no slab to nucleate earthquakes or release volatiles into the mantle wedge, while the patterns of heat flow and anomalous volcanism are surface manifestations of asthenospheric upwelling and mantle flow influenced by the geometry of the slab window.

The patterns of mantle flow in slab windows, and the degree of coupling between lithospheric deformation and asthenospheric flow, are not well understood. Seismic anisotropy is the primary tool used to study these patterns, relying on the relationship between shear strain and the crystal preferred orientation of mantle minerals to infer the direction of mantle flow (e.g., Skemer and Hansen, 2016; Karato et al., 2008). Shear wave splitting measurements have been interpreted as showing that lateral mantle flow occurs through slab windows (e.g., Russo et al., 2010a; Ben-Mansour et al., 2022; Levin et al., 2021), and geochemical evidence for material transported from distal regions through the Patago-

nian slab window further supports this hypothesis (e.g., Mallick et al., 2023). Toroidal flow around slab window edges is also suggested by observations (e.g., Ben-Mansour et al., 2022; Zandt and Humphreys, 2008; Eakin et al., 2010; Civello and Margheriti, 2004; Peyton et al., 2001) and predicted by geodynamic models (Sanhueza et al., 2023b; Jadamec and Billen, 2010; Király et al., 2017). Accurately mapping these patterns of mantle flow requires methods that are able to resolve variations in seismic anisotropy both laterally and with depth.

The Patagonian slab window is an exemplary location for studying slab window dynamics. Shear wave velocities are up to 8% slower than a global average within the slab window, indicating that the slab window promotes warmer mantle temperatures and lower mantle viscosity (Mark et al., 2022). Further, the Patagonian Icefields sit in the southernmost Andes above the slab window, and changes in surface loading associated with the growth and shrinkage of the icefields over time create a natural laboratory where the effects of the perturbed mantle viscosity structure are clearly observable in the signal of glacial isostatic adjustment (GIA) (Richter et al., 2016; Lange et al., 2014; Russo et al., 2021; Hollyday et al., 2023). Patagonia also offers an opportunity to look at the temporal evolution of slab window effects, since the Patagonian slab window has opened from south to north beneath South America as the Chile Ridge triple junction has migrated from 54°S to its current location offshore the Taitao Peninsula near 46°S (Breitsprecher and Thorkelson, 2009). Seismic mod-

*Corresponding author: hmark@ldeo.columbia.edu

els indicate that the lowest velocities in the mantle are present in the youngest part of the slab window, close to the present-day triple junction (Mark et al., 2022; Russo et al., 2010b). Shear wave splits suggest that E/W mantle flow through the Patagonian slab window has occurred, though the direction and depth of flow are unresolved; and that toroidal flow occurs around the edge of the Nazca slab at the northern edge of the slab window (Ben-Mansour et al., 2022).

Here we present an azimuthally anisotropic V_{sv} model for Patagonia, derived from Rayleigh wave measurements, which illuminates the anisotropy patterns of the upper mantle in and around the Patagonian slab window. This model focuses on shallow mantle anisotropy, complementary to shear wave splits which sense greater depths in the asthenosphere but also integrate anisotropy over a larger depth range. Anisotropy is measured in two sub-layers of the upper mantle: one from ~30-70 km depth interpreted as broadly representing the lithospheric mantle, and a second layer from ~70-200 km depth representing the asthenosphere. Lithospheric thickness varies across the study region, so a 40 km thickness for the lithospheric mantle is taken as an average value. The anisotropic fast directions from the Rayleigh waves differ from splits in most areas, indicating that the lithosphere and asthenosphere are significantly decoupled and are recording different strain histories. Closer alignment between splits and Rayleigh wave fast directions in the upper mantle below 70 km depth within the youngest part of the slab window suggests that cross-basin mantle flow is occurring in the asthenosphere.

2 Data and methods

We obtained an anisotropic shear velocity (V_{sv}) model for Patagonia by using fundamental mode Rayleigh wave dispersion curves to tomographically invert for anisotropic phase velocities, and then inverting for velocity and azimuthal anisotropy as a function of depth in a Bayesian framework. The dispersion curves were previously obtained from ambient noise (8-40 sec) and earthquake records (20-100 sec) as described in Mark et al. (2022), and the isotropic V_{sv} model from that study was also used as a starting point for the anisotropic Bayesian inversion. The product of this process is a regional model for isotropic background V_{sv} coupled with fast directions and magnitudes of 2θ azimuthal anisotropy.

2.1 Anisotropic phase velocities

Rayleigh wave dispersion curves derived from interstation traveltime measurements were inverted for azimuthally anisotropic phase velocity maps at periods between 8 and 100 seconds. The tomographic inversion used a least-squares approach (Paige and Saunders, 1982) with lateral smoothing and a small amount of norm damping, following the method of Darbyshire and Lebedev (2009). The spatial sensitivity kernels were frequency-independent, and were defined on a dense triangular grid with a knot spacing of 20 km (Lebedev

and van der Hilst, 2008; Wang and Dahlen, 1995). The model grid used a larger knot spacing of 80 km.

The Rayleigh wave tomography yielded background isotropic phase velocities and both 2θ and 4θ anisotropy magnitudes and orientations at each period (Figure 1) (Smith and Dahlen, 1973). Uncertainties were estimated by running 100 bootstrap realizations of the tomographic inversion, with each iteration using a random sample of 70% of the inter-station dispersion curves. The bootstrap analysis indicated that the best resolved periods for phase velocities were between 30 and 70 seconds. Previous studies have shown that the 4θ anisotropy terms are non-negligible, but are typically small compared to 2θ terms in the case of azimuthal anisotropy due to crystal preferred orientation (CPO) of olivine as expected for the upper mantle (Montagner and Nataf, 1986). 4θ terms are therefore included in the phase velocity tomography, but are not interpreted or included in the Bayesian inversion described below because they are likely representative, in part, of leakage between components due to imperfect data coverage and approximations for wave propagation embedded in the tomographic inversion process.

2.2 Bayesian inversion with anisotropic layers

Anisotropic phase velocities were inverted for 1D velocity-depth models at points throughout the study region using a Markov chain Monte Carlo (MCMC) method (Shen et al., 2013). The velocity-depth model at each evaluation point was described by 14 parameters for isotropic structure, and 6 parameters for anisotropic structure (Figure 2). The isotropic parameters were the thicknesses of the crust and sediment layers; top and bottom velocities for the sediment layer; four spline coefficients for the crustal layer velocities; and six spline coefficients for mantle velocities. The structure was parameterized from the surface to 300 km depth, with velocities converging to the global model AK135 from 200-300 km depth where the data do not provide constraints. Initial values for layer thicknesses, velocities, and spline coefficients were taken from an existing isotropic V_{sv} model for the region derived using an isotropic version of the same Bayesian framework (Mark et al., 2022). Velocities were required to be monotonically increasing across layer boundaries, from sediments to crust to mantle, and a maximum value of 4.9 km/s was imposed for the mantle spline coefficients. Assuming that anisotropy has a second-order effect on the overall velocity structure, the isotropic parameters should be similar between the isotropic and the anisotropic Bayesian inversions. Therefore, while the velocity gradients, spline coefficients, and layer thicknesses were allowed to vary, the prior distributions for these isotropic parameters were kept relatively narrow (Table S1).

Anisotropy was included in the crust and mantle using an approach similar to Zhou et al. (2024). The crust was parameterized as a single anisotropic layer with associated coefficients for 2θ-periodic sine and cosine terms. The mantle was divided into two sub-layers, each with a set of coefficients (Figure S9). The two mantle lay-

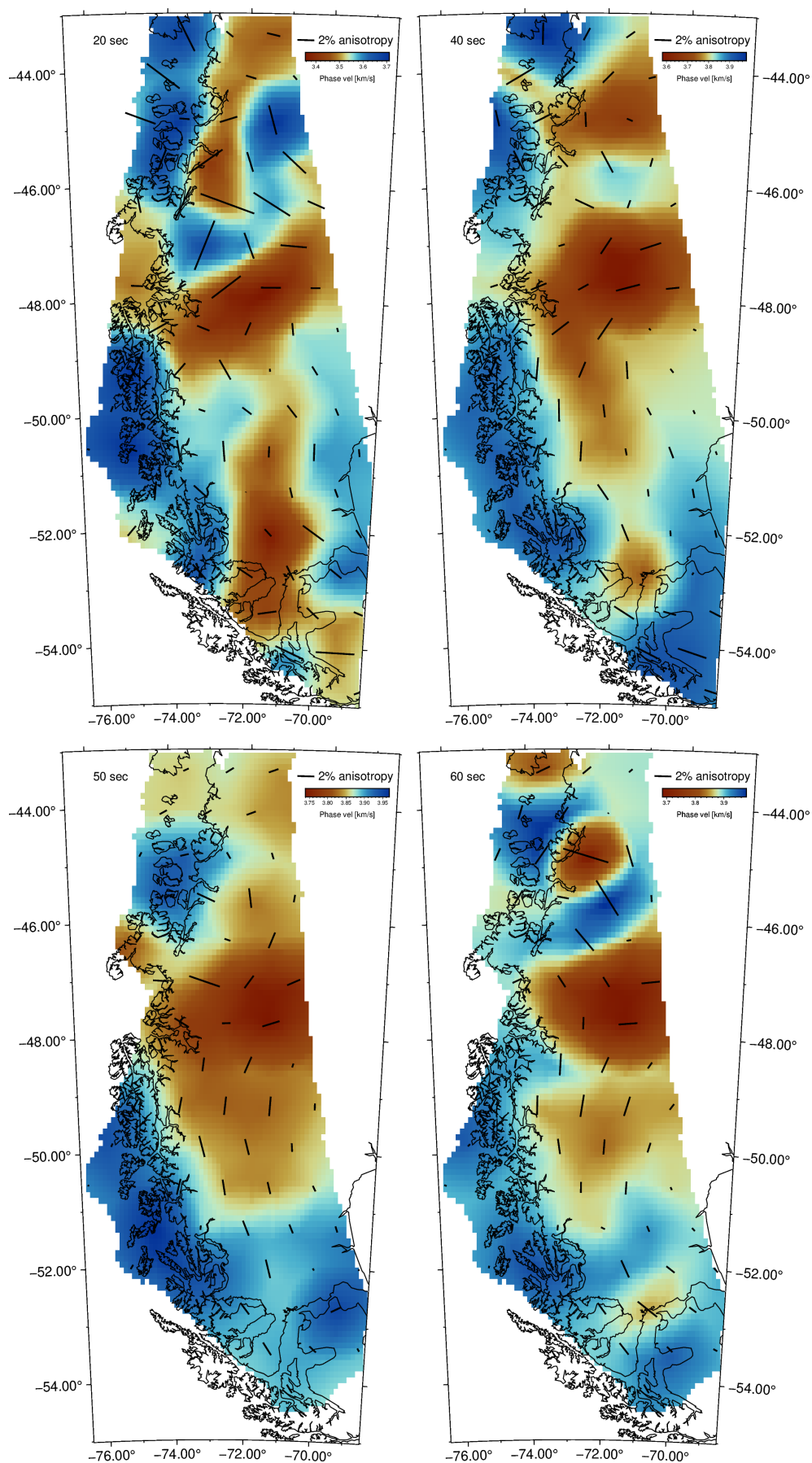**Figure 1** Phase velocity maps with 2θ anisotropy components, at 20, 40, 50, and 60 seconds period.
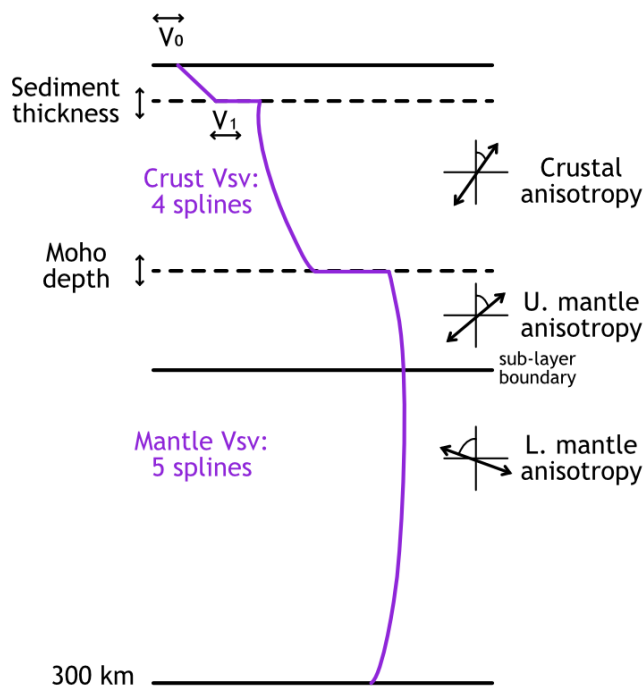
Figure 2 A diagram of the 1D model parameterization for the Bayesian MCMC inversion. Horizontal black lines denote layer or sub-layer boundaries; dashed boundaries are allowed to move in the inversion. Figure modified from Shen et al. (2013), Figure 6.

ers notionally represent the lithospheric and asthenospheric mantle. The boundary between the anisotropic mantle sub-layers was not allowed to move during inversion but several different fixed values for the thickness of the upper mantle sub-layer were tested, with 40 km taken as the preferred value approximating an average lithospheric thickness (Figure 3). To set the mantle layer thicknesses, we considered that the sensitivity of the Rayleigh wave dataset decreases sharply below ~100 km and the crust is ~30 km thick throughout the study region. Therefore, to ensure that the data still had some sensitivity to structure in the lower sub-layer, the upper sub-layer thickness was kept below 60 km. The aim was not to specifically resolve lithospheric vs asthenospheric anisotropy, but to allow for depth-varying anisotropy in an intentionally simplified model to capture regional patterns while avoiding over-parameterization. Varying the upper mantle sub-layer thickness had a small effect on the amplitude of anisotropy in each of the mantle sub-layers, but did not significantly influence the anisotropic fast directions (Figure 4). The crust might reasonably be thought to have a layered structure with, at minimum, upper and lower portions; however, since mantle anisotropy was the target of this study, a single set of anisotropy parameters was used for the entire crust to avoid over-parameterizing the problem relative to the data. Tests including two anisotropic crustal layers primarily changed the magnitude of crustal anisotropy by partitioning the signal between the upper and lower portions, similar to the effect of varying the thickness of the upper mantle sub-layer. While anisotropy was

included in inversions across the model space, in Figures 3 and 4 we only show anisotropy results where the MCMC uncertainty in the fast direction was less than 30°, which we consider the threshold for well-resolved anisotropy parameters.

3 Results

The background isotropic velocity structure obtained in this anisotropic inversion is highly similar to the isotropic structure used as a starting point for the Bayesian inversion (Mark et al., 2022) (see Figures S1-S5). This broad similarity makes sense, given that anisotropy is a second-order component of the velocity structure. The main feature of both models is the low velocity anomaly associated with the youngest part of the slab window. The two velocity models are not identical: in particular, fast velocities previously imaged beneath the Austral-Magallanes basin are less prominent in the background velocity structure of the anisotropic model. Some small differences between the isotropic and anisotropic models are expected due to anisotropy aliasing into the fully isotropic model where azimuthal coverage is not well balanced. However, the good agreement between the velocity models indicates that this aliasing is limited and the anisotropic inversion is fitting the anisotropic structure primarily to the residuals with respect to isotropic structure. The Austral-Magallanes basin is still clearly resolved in the sedimentary structure, and the crustal thickness matches the isotropic model within ±3 km in most of the region (Figures S6-S7).

Anisotropic fast directions in the upper mantle vary, defining three sub-regions within the study area: southern, northern, and central (Figure 3). In the southern sub-region, from 54°S to ~49°S, fast directions in both mantle sub-layers are approximately trench-parallel. In the northern sub-region, north of 46°S, fast directions in the upper mantle sub-layer are oriented NE/SW and directions for the lower mantle sub-layer are variable. In the central sub-region, over the youngest part of the present-day slab window, upper mantle sub-layer fast directions are mostly NE/SW, while the lower mantle sub-layer trends E/W and SE/NW.

Crustal anisotropy is small across most of the study region, with the largest amplitudes present south of 51°S and highly variable fast directions throughout. The larger amplitudes in the south may be due to the presence of thick sediments and thin crust, leaving a relatively thinner anisotropic layer in the MCMC model. Sedimentary structures within the Austral-Magallanes Basin may also influence anisotropy in complex ways that cannot be resolved at the spatial scales of this study. In the northern part of the study region, near the triple junction, crustal fast directions are similar to those measured by Gallego et al. (2011) using ambient noise at periods of 6-12 sec.

4 Discussion

Azimuthal anisotropy in Patagonia measured from Rayleigh waves at periods up to 100 sec is consistent
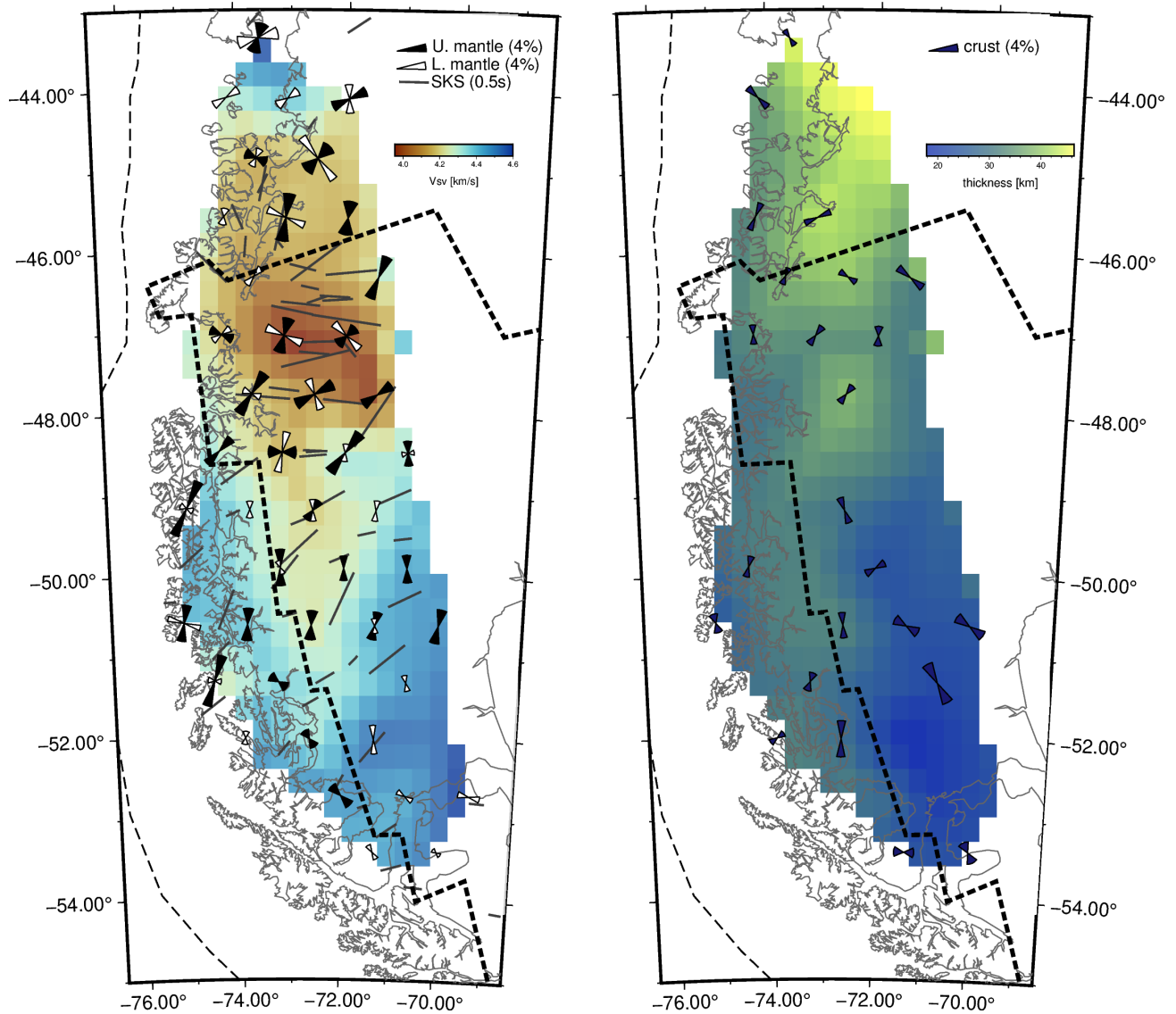
Figure 3 Anisotropy results for the preferred model from this study. Anisotropy symbols are only plotted in locations where the anisotropy is resolved (uncertainty in the fast direction $< 30°$). Thin dashed line shows the trench axis offshore; thick dashed line is the projected slab window location from Breitsprecher and Thorkelson (2009). **Left:** Mantle anisotropy in the upper and lower sub-layers, for a model where the upper mantle sub-layer is 40 km thick, along with splits from Ben-Mansour et al. (2022). Background colors show the isotropic component of V_{sv} at 60 km depth. **Right:** Crustal anisotropy for the same model. Background colors show crustal thickness in km.

with larger-scale patterns from global tomography in some but not all parts of the study region. In the global model SL2016svA, the anisotropic fast directions are oriented ~NE-SW across Patagonia down to 200 km depth (Schaeffer et al., 2016). This aligns with fast directions in the upper mantle sub-layer north of 50°S, and with some fast directions in the lower mantle sub-layer south of 48°S. Comparing global and regional tomography models in this way is difficult as their different spatial scales result in very different resolutions and levels of smoothing. However, we note that the area where the global and regional models for anisotropy differ the most is in the lower mantle sub-layer in the youngest part of the slab window, suggesting that the fast directions there deviate from larger-scale patterns of trench-parallel anisotropy or anisotropy influenced by absolute plate motion, in an area smaller than the resolution of the global model.

Crustal anisotropy is not resolved well in much of the region, but measurements near the triple junction are in good agreement with previous studies (Gallego et al., 2011). Short-period anisotropy measured near the triple junction has previously been interpreted in terms of deformation due to plate convergence, with fast directions north of the triple junction reflecting oblique convergence and the forearc sliver bounded by the Liquiñe-Ofqui fault zone, and directions further south shaped by normal convergence of the Antarctic plate.

In the southern sub-region between 54°S and 49°S, anisotropic fast directions in both mantle sub-layers are approximately trench-parallel. While the Patagonian slab window is still largely present beneath this part of South America, with the leading edge of the subducting Antarctic slab marked by adakitic volcanism in the Austral Volcanic Zone (Stern and Kilian, 1996), this region has a long history of subduction and compression along the margin prior to the slab window forming which is likely responsible for the signal observed in the shallow upper mantle (Seton et al., 2012). Trench-parallel anisotropy has been observed globally across most subduction zones, and while the origin of these signals is still debated, common interpretations include the presence of highly anisotropic serpentine mineral fabrics (Wagner et al., 2013; Katayama et al., 2009; Mookherjee and Capitani, 2011), olivine CPO formed by mantle corner flow under conditions that promote B-type fabric (Long and van der Hilst, 2006; Kneller et al., 2007; Nakajima and Hasegawa, 2004), and/or trench-parallel mantle flow driven by particular subduction geometry or slab rollback (Kneller and van Keken, 2007; Russo and Silver, 1994; Lynner and Beck, 2020) such as rollback of the Antarctic slab suggested by geodynamic models (Sanhueza et al., 2023a). In contrast, SKS splitting fast directions in southern Patagonia tend to be oriented NE/SW, oblique to the trench. These splitting orientations are interpreted as representing regional asthenospheric flow (Ben-Mansour et al., 2022; Schaeffer et al., 2016). The difference in fast directions suggests that the splits are sensing deeper structure compared to the Rayleigh waves. This is a reasonable interpretation, given that SKS splits essentially provide a measurement of anisotropy that is depth-integrated along a path

from the core-mantle boundary to a surface seismic station. The lithosphere in this region is also expected to be thick, comprising a relatively old continental block (Schilling et al., 2017), consistent with the interpretation that the Rayleigh waves here are sensing primarily lithospheric structure.

Rayleigh wave fast directions in the upper mantle in the northern sub-region again parallel the trench, indicating that subduction is controlling the anisotropic structure, similar to what is seen south of 49°S. Unlike in the south, however, the Rayleigh wave fast directions are in good agreement with shear wave splits. This may be a coincidence of geometry, with trench-parallel anisotropy in the lithosphere aligning with regional asthenospheric flow as observed in global models due to the strike of the trench in this section of the subduction zone (Schaeffer et al., 2016; Ben-Mansour et al., 2022).

In the youngest part of the slab window, between 49°S and 46°S, Rayleigh wave fast directions are primarily NE/SW in the upper mantle sub-layer, while directions in the lower mantle sub-layer are in closer alignment with shear wave splits which show consistent E/W orientations (Ben-Mansour et al., 2022; Russo et al., 2010a). While azimuthal anisotropy point measurements in the lower mantle sub-layer should be interpreted with caution as the Rayleigh wave constraints are weaker at greater depths, the stronger agreement between those fast directions and shear wave splits suggests that there is some sensitivity to flow in the asthenosphere from the longer-period Rayleigh waves in this region. Seismic models indicate that the lithosphere is thinned in the youngest part of the slab window, possibly due to thermochemical erosion, which would bring more of the asthenosphere within a depth range that the long-period Rayleigh waves are sensitive to (Mark et al., 2022). Previous studies have interpreted patterns of both anisotropy (Ben-Mansour et al., 2022; Russo et al., 2010a) and lava geochemistry (Guest et al., 2024; Mallick et al., 2023) as indicating that the mantle flows laterally through the slab window beneath South America, exchanging material between the Atlantic and Pacific basins. Modeling studies have also found that horizontal flow is likely to occur in the slab window (Sanhueza et al., 2023a; Wu et al., 2022). Taken all together, the pattern of Rayleigh wave fast directions suggests that this exchange flow occurs below the upper sub-layer such that even in an area where the lithospheric mantle is dramatically thinned, E/W mantle flow is not occurring directly beneath the crust.

It is also possible that differences between Rayleigh wave and splitting anisotropy orientations in the shallow mantle near the Chile Ridge triple junction are due in part to limitations in the inversion process and/or sparsity of data. Seismic data across Patagonia are drawn primarily from a series of temporary broadband deployments which did not overlap in time or, mostly, in space. Phase velocities derived from inter-station traveltime measurements are therefore sparse in the regions along the edges of different deployments, including the join between the GUANACO and CRSP networks near 47°S because those two arrays were not deployed at the same time (Russo et al., 2010b; Magnani et al., 2020).
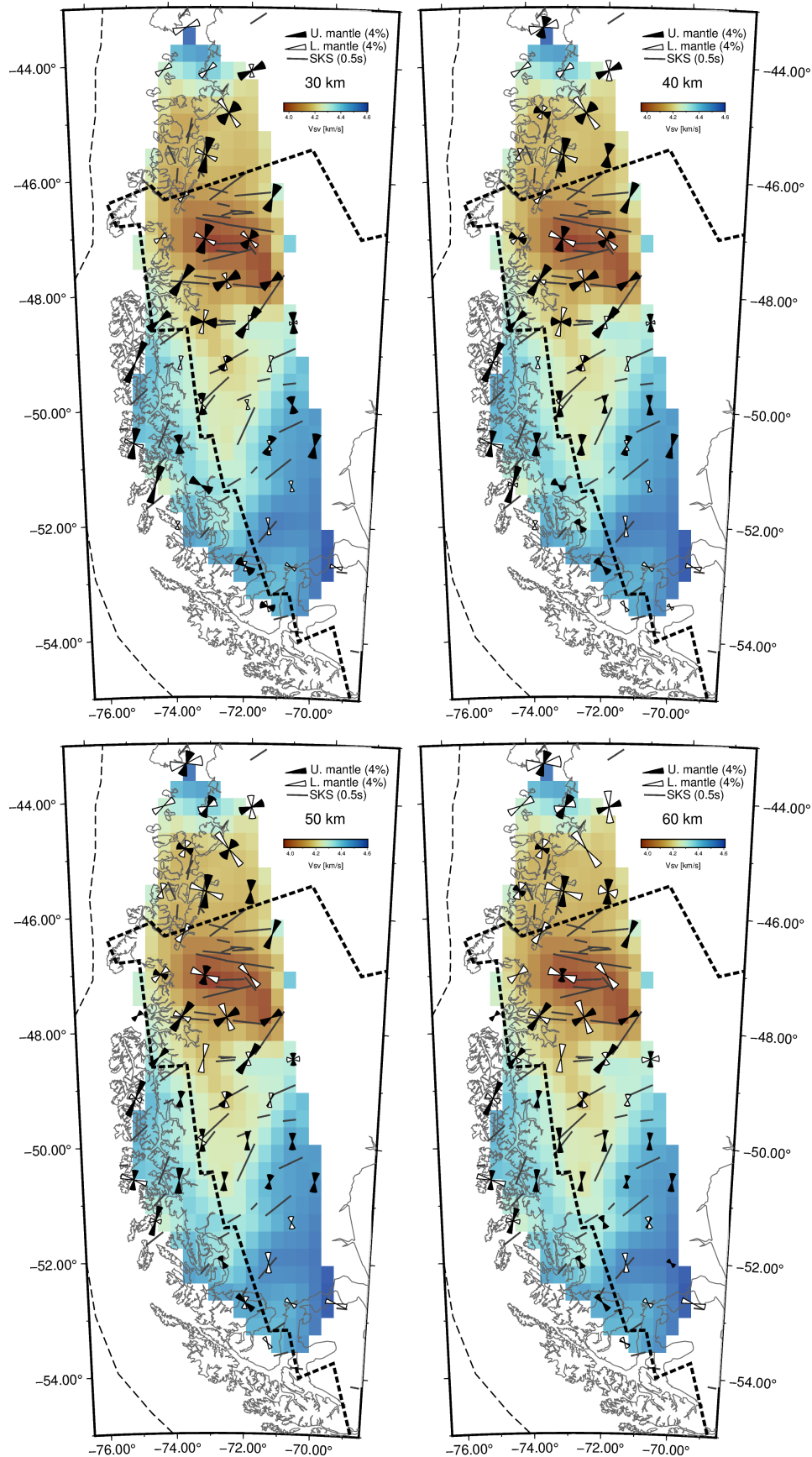
Figure 4 Mantle anisotropy in both sub-layers for models where the upper sub-layer was 30, 40, 50, or 60 km thick. Anisotropy symbols are only plotted in locations where the anisotropy is resolved (uncertainty in the fast direction < 30°). Thin dashed line shows the trench axis offshore; thick dashed line is the projected slab window location from Breitsprecher and Thorkelson (2009). Background colors show the isotropic component of V_{sv} at 60 km depth. Splits are from Ben-Mansour et al. (2022)

Having fewer phase velocity measurements with a less robust azimuthal distribution may also explain the lack of consistency across periods in 2θ fast directions in the same area (Figure 1), which in turn makes it difficult for the Bayesian inversion process to settle on a model that fits the phase velocity inputs well within the constraints of 2-layer mantle anisotropy. These caveats are important to consider, but ultimately the fast direction uncertainties from both bootstrap phase velocity inversions and the MCMC inversion suggest that the directions are reasonably well-constrained, and we therefore interpret them as representations of subsurface structure.

Differing depth sensitivities in a region of complex flow could explain results of anisotropic inversion and their differences and similarities with respect to splits. In this paradigm, the upper mantle sub-layer anisotropy reflects some combination of the history of subduction and complex present-day mantle flow, while the lower mantle sub-layer shows anisotropy related to E/W mantle flow through the slab window similar to splitting measurements.

5 Conclusions

Comparisons between these Rayleigh wave anisotropy measurements and previous shear wave splitting studies in the Patagonian slab window indicate that mantle anisotropy and, by extension, the pattern of mantle flow, varies with depth in the upper mantle. Shallow mantle anisotropy appears to reflect primarily the history of subduction and compression along the South American margin prior to the slab window opening, with trench-parallel fast directions similar to what is often observed in subduction zones globally. Trench-parallel fast directions are frequently interpreted as reflecting non-A type olivine fabric formed in the presence of water, serpentine fabric, or trench-parallel flow; with seismic data, it is not possible to distinguish between these possibilities. Below these trench-parallel fast directions, Rayleigh wave anisotropy in the youngest part of the slab window aligns more closely with E/W fast directions seen from shear wave splits. This pattern suggests that cross-basin flow through the slab window occurs in the upper mantle, within the depth range sensed by longer-period Rayleigh waves.

Both geochemical evidence and modeling results further support the hypothesis that mantle flow between the Atlantic and the Pacific is happening within the asthenospheric mantle in Patagonia. Geochemistry of erupted basalts indicates the addition of mantle components advected laterally, from beneath the South Atlantic and South America westward to backarc volcanic plateaus and the Chile Ridge (Guest et al., 2024; Mallick et al., 2023; Husson et al., 2012; Søager et al., 2021); and geodynamic models predict that horizontal mantle flow can occur through slab windows (Sanhueza et al., 2023a,b; Wu et al., 2022). Azimuthal anisotropy cannot distinguish eastward versus westward flow, and the direction of material transport in the Patagonian slab window remains a matter of debate, as some geochemical evidence favors westward flow while models of mantle dynamics suggest the flow is eastward (e.g., Mallick et al., 2023; MacDougall et al., 2014; Guillaume et al., 2010). Further study, including time-evolving 3D geodynamic models, could provide more constraints on the direction of mantle flow.

The distinction between shallow (30-70 km depth range) versus deeper (70-120 km depth) anisotropy can be thought of as reflecting the different physical conditions and strain histories of the lithosphere and asthenosphere. Lithospheric thickness likely varies throughout the region (e.g., Mark et al., 2022) in contrast to the fixed sub-layer thicknesses in this anisotropic model, but the primary patterns of anisotropy in the two mantle sub-layers nonetheless map conceptually onto lithospheric structure shaped by subduction history and asthenospheric flow, respectively. Notably, the difference in anisotropic fast directions inferred in the two mantle sub-layers suggests that mantle flow is not strongly coupled between the lithosphere and asthenosphere in the Patagonian slab window.

The complexity of mantle flow in and around the Patagonian slab window can only be partly captured by azimuthal anisotropy measurements. While azimuthal anisotropy gives us a flattened perspective on mantle flow in map view, we fully expect the flow field to be three-dimensional due both to edge effects around the subducting slabs and GIA. Future work on radial anisotropy would provide additional information on mantle dynamics in the slab window.

Acknowledgements

Data and code availability

Raw seismic data, and some processed cross-correlations, are available as described in Mark et al. (2022). The final anisotropic velocity model is available on Zenodo (Mark et al., 2025)

Competing interests

The authors have no competing interests.

References

Agurto-Detzel, H., Rietbrock, A., Bataille, K., Miller, M., Iwamori, H., and Priestley, K. Seismicity distribution in the vicinity of the Chile Triple Junction, Aysén Region, southern Chile. *Journal of South American Earth Sciences*, 51:1–11, Apr. 2014. doi: 10.1016/j.jsames.2013.12.011.

Ávila, P. and Dávila, F. M. Heat flow and lithospheric thickness analysis in the Patagonian asthenospheric windows, southern South America. *Tectonophysics*, 747-748:99–107, Nov. 2018. doi: 10.1016/j.tecto.2018.10.006.

Ben-Mansour, W., Wiens, D. A., Mark, H. F., Russo, R. M., Richter, A., Marderwald, E., and Barrientos, S. Mantle Flow Pattern Associated With the Patagonian Slab Window Determined From Azimuthal Anisotropy. *Geophysical Research Letters*, 49(18), 2022. doi: 10.1029/2022GL099871.

Bourgois, J., Lagabrielle, Y., Martin, H., Dyment, J., Frutos, J., and Cisternas, M. E. A Review on Forearc Ophiolite Obduction, Adakite-Like Generation, and Slab Window Development at the Chile Triple Junction Area: Uniformitarian Framework for Spreading-Ridge Subduction. *Pure and Applied Geophysics*, 173 (10-11):3217–3246, Oct. 2016. doi: 10.1007/s00024-016-1317-9.

Breitsprecher, K. and Thorkelson, D. J. Neogene kinematic history of Nazca–Antarctic–Phoenix slab windows beneath Patagonia and the Antarctic Peninsula. *Tectonophysics*, 464(1-4):10–20, Jan. 2009. doi: 10.1016/j.tecto.2008.02.013.

Civello, S. and Margheriti, L. Toroidal mantle flow around the Calabrian slab (Italy) from SKS splitting. *Geophysical Research Letters*, 31(10), 2004. doi: 10.1029/2004GL019607.

Darbyshire, F. A. and Lebedev, S. Rayleigh wave phase-velocity heterogeneity and multilayered azimuthal anisotropy of the Superior Craton, Ontario. *Geophysical Journal International*, 176(1): 215–234, Jan. 2009. doi: 10.1111/j.1365-246X.2008.03982.x.

DeLong, S. E., Schwarz, W., and Anderson, R. N. Thermal effects of ridge subduction. *Earth and Planetary Science Letters*, 44(2): 239–246, Aug. 1979. doi: 10.1016/0012-821X(79)90172-9.

Eakin, C. M., Obrebski, M., Allen, R. M., Boyarko, D. C., Brudzinski, M. R., and Porritt, R. Seismic anisotropy beneath Cascadia and the Mendocino triple junction: Interaction of the subducting slab with mantle flow. *Earth and Planetary Science Letters*, 297(3-4):627–632, 2010. doi: 10.1016/j.epsl.2010.07.015.

Gallego, A., Panning, M., Russo, R. M., Comte, D., Mocanu, V., Murdie, R., and Vandecar, J. Azimuthal anisotropy in the Chile Ridge subduction region retrieved from ambient noise. *Lithosphere*, 3 (6), 2011. doi: 10.1130/L139.1.

Guest, I. A., Saal, A. E., Mallick, S., Gorring, M. L., and Kay, S. M. The Volcanism of the Meseta del Lago Buenos Aires, Patagonia: the Transition from Subduction to Slab Window. *Journal of Petrology*, 65(6), June 2024. doi: 10.1093/petrology/egae052.

Guillaume, B., Moroni, M., Funiciello, F., Martinod, J., and Faccenna, C. Mantle flow and dynamic topography associated with slab window opening: Insights from laboratory models. *Tectonophysics*, 496(1), Dec. 2010. doi: 10.1016/j.tecto.2010.10.014.

Hollyday, A., Austermann, J., Lloyd, A., Hoggard, M., Richards, F., and Rovere, A. A Revised Estimate of Early Pliocene Global Mean Sea Level Using Geodynamic Models of the Patagonian Slab Window. *Geochemistry, Geophysics, Geosystems*, 24(2), 2023. doi: 10.1029/2022GC010648.

Husson, L., Conrad, C. P., and Faccenna, C. Plate motions, Andean orogeny, and volcanism above the South Atlantic convection cell. *Earth and Planetary Science Letters*, 317-318:126–135, Feb. 2012. doi: 10.1016/j.epsl.2011.11.040.

Jadamec, M. A. and Billen, M. I. Reconciling surface plate motions with rapid three-dimensional mantle flow around a slab edge. *Nature*, 465(7296):338–341, 2010. doi: 10.1038/nature09053.

Karato, S.-i., Jung, H., Katayama, I., and Skemer, P. Geodynamic Significance of Seismic Anisotropy of the Upper Mantle: New Insights from Laboratory Studies. *Annual Review of Earth and Planetary Sciences*, 36(1):59–95, May 2008. doi: 10.1146/annurev.earth.36.031207.124120.

Katayama, I., Hirauchi, K.-i., Michibayashi, K., and Ando, J.-i. Trench-parallel anisotropy produced by serpentine deformation in the hydrated mantle wedge. *Nature*, 461(7267): 1114–1117, Oct. 2009. doi: 10.1038/nature08513.

Király, Á., Capitanio, F. A., Funiciello, F., and Faccenna, C. Subduction induced mantle flow: Length-scales and orientation of the toroidal cell. *Earth and Planetary Science Letters*, 479:284–297, 2017. doi: 10.1016/j.epsl.2017.09.017.

Kneller, E. A. and van Keken, P. E. Trench-parallel flow and seismic anisotropy in the Mariana and Andean subduction systems. *Nature*, 450(7173):1222–1225, Dec. 2007. doi: 10.1038/nature06429.

Kneller, E. A., van Keken, P. E., Katayama, I., and Karato, S. Stress, strain, and B-type olivine fabric in the fore-arc mantle: Sensitivity tests using high-resolution steady-state subduction zone models. *Journal of Geophysical Research: Solid Earth*, 112(B4), Apr. 2007. doi: 10.1029/2006JB004544.

Lange, H., Casassa, G., Ivins, E. R., Schröder, L., Fritsche, M., Richter, A., Groh, A., and Dietrich, R. Observed crustal uplift near the Southern Patagonian Icefield constrains improved viscoelastic Earth models. *Geophysical Research Letters*, 41(3): 805–812, Feb. 2014. doi: 10.1002/2013GL058419.

Lebedev, S. and van der Hilst, R. D. Global upper-mantle tomography with the automated multimode inversion of surface and S-wave forms. *Geophysical Journal International*, 173(2):505–518, May 2008. doi: 10.1111/j.1365-246X.2008.03721.x.

Levin, V., Elkington, S., Bourke, J., Arroyo, I., and Linkimer, L. Seismic anisotropy in southern Costa Rica confirms upper mantle flow from the Pacific to the Caribbean. *Geology*, 49(1):8–12, Jan. 2021. doi: 10.1130/G47826.1.

Long, M. D. and van der Hilst, R. D. Shear wave splitting from local events beneath the Ryukyu arc: Trench-parallel anisotropy in the mantle wedge. *Physics of the Earth and Planetary Interiors*, 155(3), May 2006. doi: 10.1016/j.pepi.2006.01.003.

Lynner, C. and Beck, S. L. Subduction dynamics and structural controls on shear wave splitting along the South American convergent margin. *Journal of South American Earth Sciences*, 104, 2020. doi: 10.1016/j.jsames.2020.102824.

MacDougall, J. G., Kincaid, C., Szwaja, S., and Fischer, K. M. The impact of slab dip variations, gaps and rollback on mantle wedge flow: insights from fluids experiments. *Geophysical Journal International*, 197(2):705–730, May 2014. doi: 10.1093/gji/ggu053.

Magnani, M. B., Ito, E., Wiens, D., Wickert, A. D., Ivins, E. R., Fedotova, A., Van Wyk de Vries, M. S., Mark, H. F., and Penprase, S. B. Solid Earth response of the Patagonian Andes to post-Little Ice Age glacial retreat: a multi-pronged approach. *AGU Fall Meeting Abstracts*, pages G013–05, Dec. 2020. https://ui.adsabs.harvard.edu/abs/2020AGUFMG013...05M.

Mallick, S., Kuhl, S. E., Saal, A. E., Klein, E. M., Bach, W., Monteleone, B. D., and Boesenberg, J. S. Evidence of South American lithosphere mantle beneath the Chile mid-ocean ridge. *Earth and Planetary Science Letters*, 620:118320, Oct. 2023. doi: 10.1016/j.epsl.2023.118320.

Mark, H., Wiens, D. A., Ben Mansour, W., and Zhou, Z. Anisotropic Vsv model for the crust and upper mantle in southern Patagonia, 2025. doi: 10.5281/zenodo.15097717. Zenodo repository.

Mark, H. F., Wiens, D. A., Ivins, E. R., Richter, A., Ben Mansour, W., Magnani, M. B., Marderwald, E., Adaros, R., and Barrientos, S. Lithospheric Erosion in the Patagonian Slab Window, and Implications for Glacial Isostasy. *Geophysical Research Letters*, 49 (2), Jan. 2022. doi: 10.1029/2021GL096863.

Montagner, J.-P. and Nataf, H.-C. A simple method for inverting the azimuthal anisotropy of surface waves. *Journal of Geophysical Research: Solid Earth*, 91(B1):511–520, 1986. http://

onlinelibrary.wiley.com/doi/10.1029/JB091iB01p00511/full.

Mookherjee, M. and Capitani, G. C. Trench parallel anisotropy and large delay times: Elasticity and anisotropy of antigorite at high pressures. *Geophysical Research Letters*, 38(9), May 2011. doi: 10.1029/2011GL047160.

Nakajima, J. and Hasegawa, A. Shear-wave polarization anisotropy and subduction-induced flow in the mantle wedge of northeastern Japan. *Earth and Planetary Science Letters*, 225 (3), Sept. 2004. doi: 10.1016/j.epsl.2004.06.011.

Paige, C. C. and Saunders, M. A. LSQR: An Algorithm for Sparse Linear Equations and Sparse Least Squares. *ACM Transactions on Mathematical Software*, 8(1):43–71, Mar. 1982. doi: 10.1145/355984.355989.

Peyton, V., Levin, V., Park, J., Brandon, M., Lees, J., Gordeev, E., and Ozerov, A. Mantle flow at a slab edge: Seismic anisotropy in the Kamchatka Region. *Geophysical Research Letters*, 28(2): 379–382, 2001. doi: 10.1029/2000GL012200.

Richter, A., Ivins, E. R., Lange, H., Mendoza, L., Schröder, L., Hormaechea, J., Casassa, G., Marderwald, E., Fritsche, M., Perdomo, R., Horwath, M., and Dietrich, R. Crustal deformation across the Southern Patagonian Icefield observed by GNSS. *Earth and Planetary Science Letters*, 452:206–215, Oct. 2016. doi: 10.1016/j.epsl.2016.07.042.

Russo, R. M. and Silver, P. G. Trench-parallel Flow Beneath the Nazca Plate from Seismic Anisotropy. *Science*, 263(5150), 1994. doi: 10.1126/science.263.5150.1105.

Russo, R. M., Gallego, A., Comte, D., Mocanu, V., Murdie, R., and VanDecar, J. Source-side shear wave splitting and upper mantle flow in the Chile Ridge subduction region. *Geology*, 38(8): 707–710, Aug. 2010a. doi: 10.1130/G30920.1.

Russo, R. M., VanDecar, J. C., Comte, D., Mocanu, V. I., Gallego, A., and Murdie, R. E. Subduction of the Chile Ridge: Upper mantle structure and flow. *GSA Today*, pages 4–10, 2010b. doi: 10.1130/GSATG61A.1.

Russo, R. M., Luo, H., Wang, K., Ambrosius, B., Mocanu, V., He, J., James, T., Bevis, M., and Fernandes, R. Lateral variation in slab window viscosity inferred from global navigation satellite system (GNSS)–observed uplift due to recent mass loss at Patagonia ice fields. *Geology*, 2021. doi: 10.1130/G49388.1.

Sanhueza, J., Yáñez, G., Buck, W. R., Araya Vargas, J., and Veloso, E. Ridge Subduction: Unraveling the Consequences Linked to a Slab Window Development Beneath South America at the Chile Triple Junction. *Geochemistry, Geophysics, Geosystems*, 24(9): e2023GC010977, Sept. 2023a. doi: 10.1029/2023GC010977.

Sanhueza, J., Yáñez, G., Buck, W. R., Sawant, A. D., Araya Vargas, J., and Lloyd, A. J. Towards linking slab window geodynamics with the geophysical and geochemical signature of the upper mantle. *Earth and Planetary Science Letters*, 623, 2023b. doi: 10.1016/j.epsl.2023.118435.

Schaeffer, A., Lebedev, S., and Becker, T. Azimuthal seismic anisotropy in the Earth's upper mantle and the thickness of tectonic plates. *Geophysical Journal International*, 207(2):901–933, Nov. 2016. doi: 10.1093/gji/ggw309.

Schilling, M. E., Carlson, R. W., Tassara, A., Conceição, R. V., Bertotto, G. W., Vásquez, M., Muñoz, D., Jalowitzki, T., Gervasoni, F., and Morata, D. The origin of Patagonia revealed by Re-Os systematics of mantle xenoliths. *Precambrian Research*, 294, 2017. doi: 10.1016/j.precamres.2017.03.008.

Seton, M., Müller, R., Zahirovic, S., Gaina, C., Torsvik, T., Shephard, G., Talsma, A., Gurnis, M., Turner, M., Maus, S., and Chandler, M. Global continental and ocean basin reconstructions since 200Ma. *Earth-Science Reviews*, 113(3-4), 2012. doi: 10.1016/j.earscirev.2012.03.002.

Shen, W., Ritzwoller, M. H., Schulte-Pelkum, V., and Lin, F.-C. Joint inversion of surface wave dispersion and receiver functions: a Bayesian Monte-Carlo approach. *Geophysical Journal International*, 192(2):807–836, Feb. 2013. doi: 10.1093/gji/ggs050.

Skemer, P. and Hansen, L. N. Inferring upper-mantle flow from seismic anisotropy: An experimental perspective. *Tectonophysics*, 668-669:1–14, Feb. 2016. doi: 10.1016/j.tecto.2015.12.003.

Smith, M. L. and Dahlen, F. A. The azimuthal dependence of Love and Rayleigh wave propagation in a slightly anisotropic medium. *Journal of Geophysical Research*, 78(17):3321–3333, June 1973. doi: 10.1029/JB078i017p03321.

Stern, C. R. and Kilian, R. Role of the subducted slab, mantle wedge and continental crust in the generation of adakites from the Andean Austral Volcanic Zone. *Contributions to Mineralogy and Petrology*, 123(3), Apr. 1996. doi: 10.1007/s004100050155.

Søager, N., Holm, P. M., Massaferro, G. I., Haller, M., and Traun, M. K. The Patagonian intraplate basalts: A reflection of the South Atlantic convection cell. *Gondwana Research*, 91, Mar. 2021. doi: 10.1016/j.gr.2020.12.008.

Thorkelson, D. J. Subduction of diverging plates and the principles of slab window formation. *Tectonophysics*, 255(1-2):47–63, Apr. 1996. doi: 10.1016/0040-1951(95)00106-9.

Wagner, L. S., Fouch, M. J., James, D. E., and Long, M. D. The role of hydrous phases in the formation of trench parallel anisotropy: Evidence from Rayleigh waves in Cascadia. *Geophysical Research Letters*, 40(11), June 2013. doi: 10.1002/grl.50525.

Wang, Z. and Dahlen, F. A. Spherical-spline parameterization of three-dimensional earth models. *Geophysical Research Letters*, 22(22):3099–3102, Nov. 1995. doi: 10.1029/95GL03080.

Wu, Y., Liao, J., Guo, F., Wang, X., and Shen, Y. Styles of Trench-Parallel Mid-Ocean Ridge Subduction Affect Cenozoic Geological Evolution in Circum-Pacific Continental Margins. *Geophysical Research Letters*, 49(8), Apr. 2022. doi: 10.1029/2022GL098428.

Zandt, G. and Humphreys, E. Toroidal mantle flow through the western U.S. slab window. *Geology*, 36(4):295, 2008. doi: 10.1130/G24611A.1.

Zhou, Z., Wiens, D. A., Nyblade, A. A., Aster, R. C., Wilson, T., and Shen, W. Crustal and Uppermost Mantle Azimuthal Seismic Anisotropy of Antarctica From Ambient Noise Tomography. *Journal of Geophysical Research: Solid Earth*, 129(1): e2023JB027556, Jan. 2024. doi: 10.1029/2023JB027556.